

Over three millennia of mercury pollution in the Peruvian Andes

Colin A. Cooke^{a,1}, Prentiss H. Balcom^b, Harald Biester^c, and Alexander P. Wolfe^a

^aDepartment of Earth and Atmospheric Sciences, University of Alberta, Edmonton, AB, Canada T6G 2E3; ^bDepartment of Marine Sciences, University of Connecticut, Groton, CT 06340; and ^cInstitute of Environmental Geology, Technical University of Braunschweig, Pockelsstrasse 3, 38106 Braunschweig, Germany

Edited by Mark Brenner, University of Florida, Gainesville, FL, and accepted by the Editorial Board April 13, 2009 (received for review January 16, 2009)

We present unambiguous records of preindustrial atmospheric mercury (Hg) pollution, derived from lake-sediment cores collected near Huancavelica, Peru, the largest Hg deposit in the New World. Intensive Hg mining first began ca. 1400 BC, predating the emergence of complex Andean societies, and signifying that the region served as a locus for early Hg extraction. The earliest mining targeted cinnabar (HgS) for the production of vermillion. Pre-Colonial Hg burdens peak ca. 500 BC and ca. 1450 AD, corresponding to the heights of the Chavín and Inca states, respectively. During the Inca, Colonial, and industrial intervals, Hg pollution became regional, as evidenced by a third lake record \approx 225 km distant from Huancavelica. Measurements of sediment-Hg speciation reveal that cinnabar dust was initially the dominant Hg species deposited, and significant increases in deposition were limited to the local environment. After conquest by the Inca (ca. 1450 AD), smelting was adopted at the mine and Hg pollution became more widely circulated, with the deposition of matrix-bound phases of Hg predominating over cinnabar dust. Our results demonstrate the existence of a major Hg mining industry at Huancavelica spanning the past 3,500 years, and place recent Hg enrichment in the Andes in a broader historical context.

cinnabar | Inca | Chavín | vermillion

Cinnabar (HgS) is the primary mineralogical source of mercury (Hg), and forms a bright red pigment (vermillion) when powdered. In the Andes, the use of vermillion is closely tied to that of precious metals, and vermillion has been recovered in burials of the elite from the first (Chavín) to the last (Inca) Andean empires, where it was used as either a body paint or a covering on ceremonial gold objects (1). During the Colonial era (1532–1900 AD), large-scale Hg mining began in earnest with the invention of Hg amalgamation in 1554 AD (2). For the next 350 years, Hg amalgamation became the dominant silver processing technique because it allowed for the extraction of silver from low-grade ores (2, 3). Nriagu (2, 3) estimated Colonial Hg emissions totalled 196,000 tons, averaging \approx 600 tons \cdot year $^{-1}$; approximately equivalent to current emissions from China (4). Estimates of Colonial Hg emissions represent minimum values for the region because they only incorporate state-registered Hg used during amalgamation. Hg emissions associated with early Hg mining therefore remain entirely unknown. Huancavelica, in the central Peruvian Andes, served as the single largest supplier of Hg to New World Colonial silver mines, and thus represents a potentially major source of preindustrial Hg pollution.

Study Region

Huancavelica is on the eastern slope of the Cordillera Occidental in central Peru (Fig. 1). Hg deposits are related to high-grade Cenozoic magmatism intruding Mesozoic and Cenozoic sedimentary rocks. Cinnabar is the dominant mercuric ore, and $>90\%$ of historically documented cinnabar production has been from the Santa Bárbara mine, immediately south of Huancavelica (5). Frequent cave-ins and extensive Hg poisoning throughout Huancavelica's 450-year Colonial history have made

it one of the most sinister examples of human exploitation and disastrous mining environments ever documented, earning it the nickname *mina de la muerte* (mine of death) (5, 6).

We recovered lake-sediment cores from 3 lakes to reconstruct the history of mining at Huancavelica. Two of the study lakes presented here are named Laguna Yanacocha (hereafter LY1 and LY2; see Fig. 1). LY1 is 10 km southeast of Huancavelica, whereas LY2 is \approx 6 km southwest and is directly up-valley from Huancavelica and the Santa Bárbara mine. Both lakes are small (LY1: 0.03 km 2 ; LY2: 0.05 km 2) and relatively deep (maximum depths for LY1: 14 m; LY2: 11 m) headwater tarns that occupy undisturbed catchments of 0.71 km 2 and 0.31 km 2 , respectively. Laguna Negrilla (hereafter Negrilla) is \approx 225 km east of Huancavelica in the Cordillera Vilcabamba (Fig. 1A). There are no major Hg deposits or mining centres in this latter region. Negrilla is a small (0.06 km 2), deep (33 m) headwater lake that occupies an undisturbed catchment of 0.32 km 2 . Lakes with undisturbed catchments were deliberately targeted to minimize confounding impacts associated with catchment disturbance, and to maximize sensitivity to atmospheric deposition of Hg.

Sediment cores were recovered from the deepest part of each lake, using a percussion corer fitted with a 7-cm-diameter polycarbonate tube. Cores were extruded into continuous 0.5-cm intervals in the field. At all 3 lakes, sediment excess ^{210}Pb activities decline in near-monotonic fashion (Table S1). To constrain ages beyond the limit of ^{210}Pb , accelerator mass spectrometry (AMS) ^{14}C measurements of discrete carbonized grass macrofossils were obtained on 5 samples from LY1, 3 samples from LY2, and 3 samples from Negrilla (Fig. 2 and Table S2). AMS ^{14}C ages were calibrated using SHCal04 (7) within Calib 5.0 (8). Concentrations of total Hg were determined on a DMA80 direct mercury analyzer (Table S3). Measurements of sediment-Hg speciation were done by solid-phase Hg thermodesorption (9), which produces temperature-dependent Hg release curves enabling identification of species such as Hg 0 , matrix-bound Hg, and inorganic HgS by comparison with reference materials (Fig. S4).

Results and Discussion

Despite different sedimentation rates (Fig. 2), the LY1 and LY2 geochemical profiles are highly concordant (Fig. 3) when plotted on their respective age-depth models. For approximately 1 millennium before ca. 1600 BC, Hg accumulation within LY2 sediment is stable and low, averaging $6 (\pm 1) \mu\text{g}\cdot\text{m}^{-2}\cdot\text{year}^{-1}$. This represents the natural, background accumulation of nonpollution Hg within LY2 sediment. The Hg profile of the Negrilla core

Author contributions: C.A.C. designed research; C.A.C., P.H.B., H.B., and A.P.W. performed research; H.B. contributed new reagents/analytic tools; C.A.C., P.H.B., H.B., and A.P.W. analyzed data; and C.A.C., P.H.B., H.B., and A.P.W. wrote the paper.

The authors declare no conflict of interest.

This article is a PNAS Direct Submission. M.B. is a guest editor invited by the Editorial Board.

¹To whom correspondence should be addressed. E-mail: cacooke@ualberta.ca.

This article contains supporting information online at www.pnas.org/cgi/content/full/0900517106/DCSupplemental.

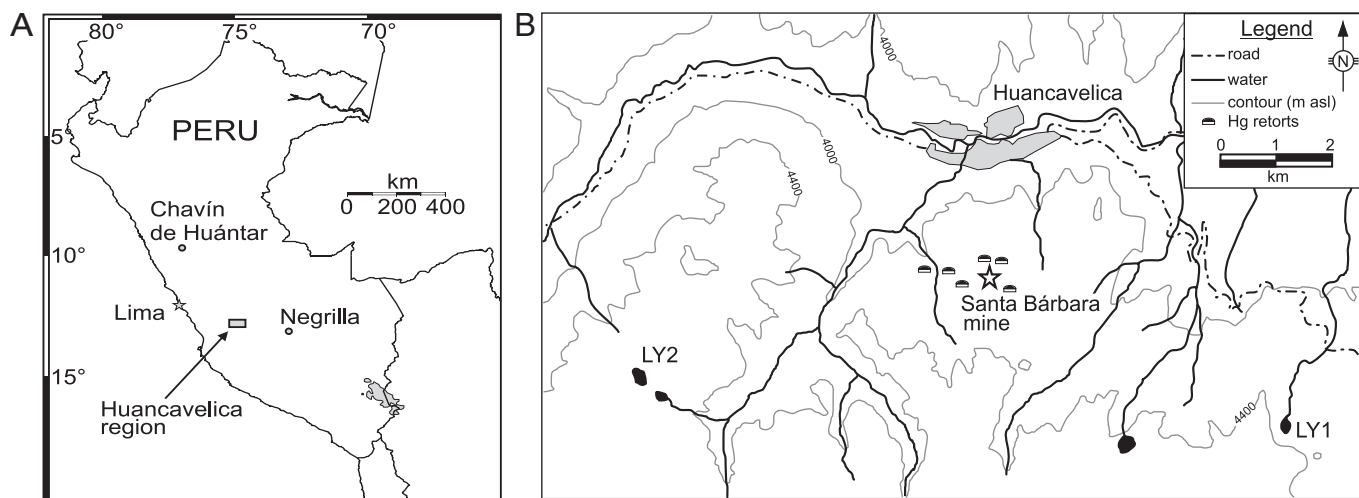


Fig. 1. Map of the study region. (A) Map of Peru with study region and location of Negrilla. (B) Detailed map of Huancavelica region with locations of Santa Bárbara mine, the 2 study lakes (LY1 and LY2), and remains of Colonial Hg retorts.

is somewhat different; however, background Hg accumulation rates are of similar magnitude [$7 (\pm 2) \mu\text{g}\cdot\text{m}^{-2}\cdot\text{year}^{-1}$] for much of this lake's early record. Background Hg levels do not appear to have been reached at LY1, although Hg accumulation rates of $6 \mu\text{g}\cdot\text{m}^{-2}\cdot\text{year}^{-1}$ are noted in the deepest intervals (Fig. 3). Thus,

we conclude that the accumulation of natural, nonpollution Hg in these lakes is $6\text{--}7 \mu\text{g}\cdot\text{m}^{-2}\cdot\text{year}^{-1}$. Although this range is consistent with nearly all other lake-sediment reconstructions of preanthropogenic Hg deposition from around the globe (10), mechanisms such as catchment export and sediment focusing ultimately serve to confound reconstructions of Hg deposition to varying degrees (11). Therefore, to enable comparability between these, and other lake-core records, sample to background flux ratios were calculated for each lake (Fig. 3).

At both LY1 and LY2, dramatic increases in Hg accumulation rates are initiated *ca.* 1400 BC, and by 600 BC both lakes exceed background by ≈ 10 -fold (Fig. 3). The accumulation of Hg subsequently decreases in both lakes until *ca.* 1200 AD at LY1 and *ca.* 1450 AD at LY2, before increasing once again. By the mid-16th century, sediment Hg accumulation rates at LY1 and LY2 are enriched by factors of ≈ 55 and ≈ 70 relative to background, respectively (Fig. 3). Only the latter increase in Hg deposition is preserved at Negrilla, where Hg accumulation rates rise dramatically *ca.* 1400 AD to over ≈ 30 times background. After 1600 AD, the Hg records for all 3 lakes are all characterized by Hg accumulation rates and flux ratios well above background (Fig. 3).

The earliest (*ca.* 1400 BC) rise in Hg at LY1 and LY2 is characterized by a 3- to 5-fold increase in Hg accumulation (Fig. 3), and occurs during a period of stable sedimentation with respect to both organic and inorganic sediment fractions (Fig. S1 and Fig. S2). Consequently, these increases cannot be explained by a rapid influx of catchment material or enhanced Hg scavenging by organic matter. Moreover, lake sediment burdens of total Hg are largely unaffected by diagenetic processes (12, 13), and represent minimum estimates of total Hg deposited to a lake surface because of reductive losses before final burial (14). Because we know of no natural mechanism capable of replicating such large and synchronized increases in Hg deposition in 2 adjacent lakes, and given their proximity to a major cinnabar deposit, we attribute with confidence the early increases of Hg observed at LY1 and LY2 to the emergence of regional-scale cinnabar mining at Huancavelica.

Less than 20 km from Huancavelica, the archaeological site of Atalla is the earliest example of large-scale ceremonial architecture in the central Andes. Although Atalla lacks direct dating and excavation, surface remains suggest the site served as a regional Center for procuring and distributing cinnabar (15). Ceramics suggest Atalla dates to the Early Horizon (*ca.* 800–300

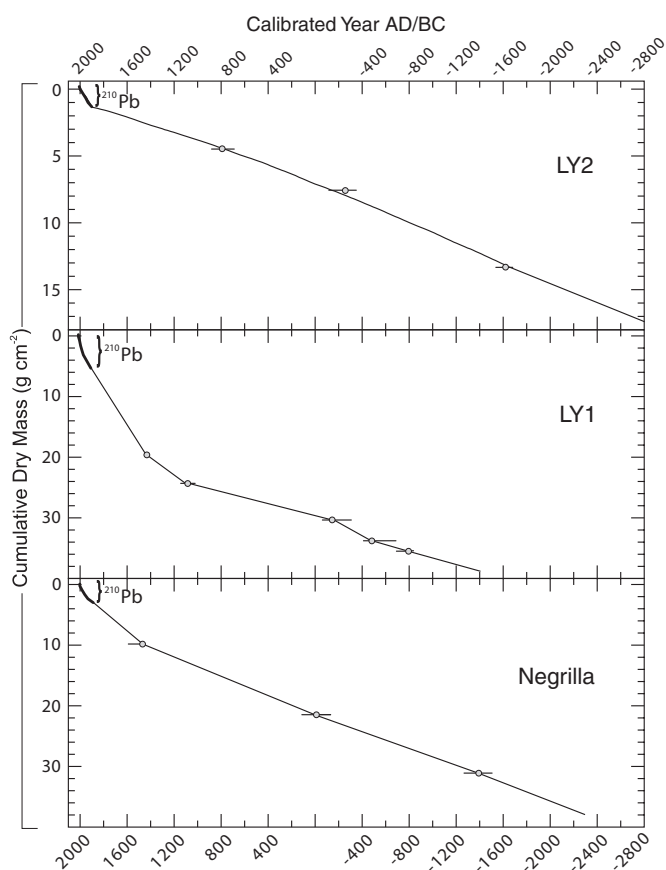


Fig. 2. Age models for the 3 lake-sediment cores. Age models for LY1 and Negrilla are based on linear interpolation between ^{210}Pb dates and median ages of calibrated ^{14}C dates, whereas a best-fit line was used between dates at LY2. AMS ^{14}C ages were measured on terrestrial charcoal and calibrated age ranges are 2σ .

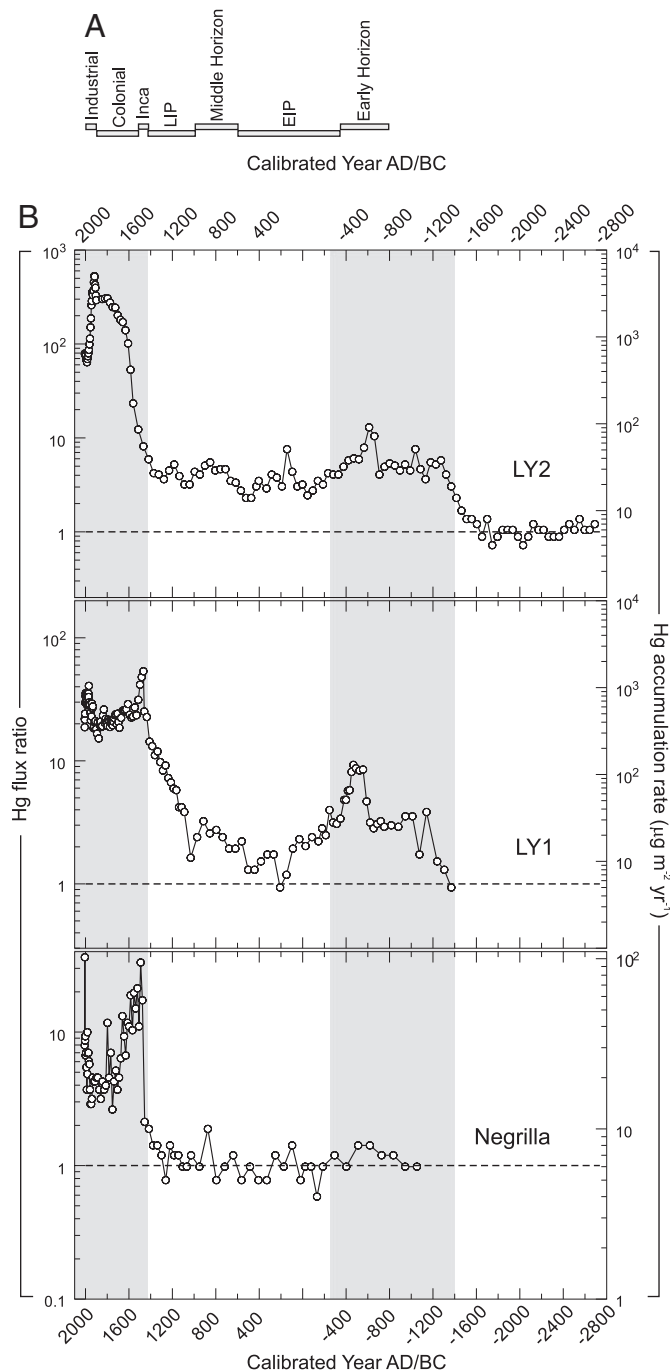


Fig. 3. Lake-sediment profiles of Hg deposition and Andean archaeology. (A) Compilation of central Andean archaeology (EIP, Early Intermediate Period; LIP, Late Intermediate Period). (B) Profiles of Hg accumulation rates and flux ratios for lakes LY2, LY1, and Negrilla. Two intervals of marked Hg enrichment are shaded. Pre-Colonial Hg deposition peaks during the height of the Chavín culture, whereas the later rise occurs under Inca and subsequent Colonial control. This second period of extensive mining activity witnessed the long-range transport of Hg emissions, as shown by the onset of Hg deposition to Negrilla, ≈ 250 km east of Huancavelica.

BC), and was actively engaged in trade with Chavín de Huántar in the Cordillera Blanca (15) (Fig. 1). Chavín influenced much of the Peruvian Andes at its apogee, and represents the cradle of complex Andean culture (16, 17). High-status burials at Chavín de Huántar, and other Early Horizon sites, commonly contain prestigious materials including gold adorned with ver-

million (17, 18). However, cinnabar mining at Huancavelica precedes even the earliest radiocarbon dates for Chavín (1), and therefore must predate the rise and expansion of Chavín culture.

The rate of Hg accumulation at both LY1 and LY2 declined during the subsequent Early Intermediate Period (*ca.* 200 BC to 500 AD; Fig. 3). At LY1, Hg flux ratios briefly return to background *ca.* 200 AD; however, no parallel return to background is evident at LY2. This discrepancy likely indicates that watershed-scale Hg retention times vary between the 2 lakes. The steady export of legacy Hg from the catchment of LY2 may be therefore partially responsible for the maintenance of elevated Hg accumulation during this period. In any case, cinnabar mining does appear to have continued during the Early Intermediate Period, although at reduced intensity. Although the collapse of Chavín likely curtailed the demand for exotic goods including cinnabar, highly stratified cultures from the north coast of Peru, such as the Moche (*ca.* 100–700 AD) and Sicán (*ca.* 700–1200 AD), may have sustained some level of imperial demand for cinnabar. Burials of Moche and Sicán nobles are some of the richest yet excavated in Peru, and vermilion is ubiquitous (19). Huancavelica is the likely source, given the scarcity of other cinnabar deposits in the Andes (20).

By 800 AD, a brief renewal in cinnabar mining is indicated as Hg flux ratios increase to 3.5 and 5.5 at LY1 and LY2, respectively (Fig. 3). This increase occurs during the Middle Horizon (*ca.* 500 to 1000 AD), and is followed by larger increases in Hg deposition at LY1 during the Late Intermediate Period (from *ca.* 1000 to 1400 AD). The Middle Horizon and the Late Intermediate Period witnessed the rapid development and expansion of mining and metallurgy in the Andes (21, 22). During the Late Intermediate Period, the archaeological site of Attalla appears to have been reoccupied (15), suggesting continuation, if not intensification, of local cinnabar processing. Inca expansion into the central Andes occurred *ca.* 1450 AD, and cinnabar production appears to have increased dramatically under Inca control. Hg accumulation at LY1 increases rapidly (>55 -fold), and is matched by the first increase in Hg at Negrilla, which exceeds background by ≈ 30 -fold (Fig. 3). The appearance of Hg pollution at Negrilla indicates Inca exploitation of the Huancavelica cinnabar deposits exceeded all previous cultures, producing a broadly dispersed legacy of Hg pollution captured by all 3 study lakes.

Inca mining continued until 1564 AD when the Spanish crown assumed control, at which time the Santa Bárbara mine was established. In contrast to cinnabar extraction for vermilion, Spanish efforts concentrated on supplying elemental Hg (Hg^0) to Colonial silver mines for use in Hg amalgamation. Hg amalgamation was invented in 1554 AD by Bartolomé de Medina in Mexico, and is considered one of the most remarkable technological advances of Ibero-America (2). Cinnabar ores from Huancavelica were smelted in grass-fired, clay-lined retorts (*hornos*; Fig. 1), until vaporization yielded gaseous Hg^0 , a portion of which was trapped in a crude condenser and cooled, yielding liquid Hg^0 . Emissions of Hg thus occurred both during mining, as cinnabar dust, but also during cinnabar smelting, as gaseous Hg^0 . Historical records of Hg production at Huancavelica indicate declining Hg output while under Colonial control, and into the 20th Century (5). At LY1 and Negrilla, Hg accumulation decreases through the Colonial period, while increasing at LY2 (Fig. 3). The apparent discordance between the Hg profiles appears to support the suggestion that the watershed of LY2 continued to export legacy Hg to the lake during periods of declining atmospheric deposition, a mechanism that has also been observed in modern lake systems (23). The mine was permanently closed in 1975 AD, and currently the only mining of Hg at Huancavelica is artisanal. In response, Hg flux ratios at Negrilla have declined, and are currently ≈ 4.6 times background in the uppermost sediments (Fig. 3). This level of relative Hg enrichment is in agreement with the vast majority of sediment-

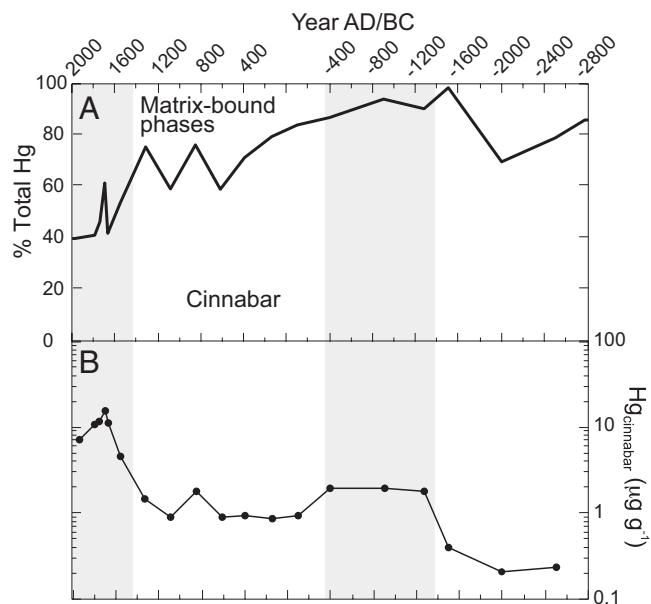


Fig. 4. Measurements of Hg speciation within LY2 sediment. (A) Plot of relative percentage cinnabar and matrix-bound phases of Hg. (B) Concentration of Hg as cinnabar down-core. Before anthropogenic enrichment a combination of cinnabar dust and matrix-bound Hg make up the sediment Hg record. During the height of Chavin mining (ca. 400–800 BC), cinnabar dust was the vast majority of sediment Hg. After Inca control of the mine (ca. 1450 AD), matrix-bound phases of Hg predominate, despite a synchronous rise in the concentration of Hg as cinnabar. This relationship suggests a shift in the phase of Hg emitted, from cinnabar dust to Hg^0 (or possibly Hg^{2+}). Both would subsequently be available for oxidation/reduction cycling within the atmosphere, sorption by organic matter, methylation, and subsequent bioaccumulation within aquatic food-webs.

core studies from remote lakes, which collectively suggest an average increase in global Hg deposition rates of 3–5x background values (10). In contrast, Hg flux ratios at both LY1 and LY2 in 1975 AD were 105 times background. Although modern flux ratios at LY1 have declined by $\approx 60\%$ (to 42 times background), no such decline is recorded at LY2. The elevated Hg accumulation rates still present at these lakes likely reflect the legacy of $>3,500$ years of regional Hg pollution residing within their catchments.

The mercuric species emitted during Colonial and pre-Colonial mining activities have direct implications for the size of the impacted airshed. Atmospheric Hg^0 has long atmospheric residence times (≈ 0.5 –1.5 years) and is the most important Hg species at the global scale (24). In contrast, oxidized reactive species of mercury can be rapidly scavenged from the atmosphere, whereas coarse particulate forms (including cinnabar dust) predominate in direct proximity to Hg point-sources (25). Measurements of Hg speciation within LY2 sediments confirm that major changes in Hg extractive technology occurred at Huancavelica (Fig. S4). Solid-phase thermal desorption reveals 2 predominant Hg phases: cinnabar and noncinnabar (i.e., matrix-bound), which are variably expressed down-core (Fig. 4). During the pre-Inca era, cinnabar was the dominant Hg species in all sediment samples, averaging 78% of the total sediment Hg inventory. Although not precluding the emission of other species

of Hg, these results suggest that pre-Inca Hg pollution, although important locally, exerted little influence beyond the range of particulate dust transport, a conclusion supported by the apparent lack of any pre-Inca Hg pollution at Negrilla. A progressive decline in the cinnabar fraction is noted in sediments that postdate ca. 1450 AD, and the majority of sediment Hg burdens remain matrix-bound through the remainder of the LY2 sediment record. This is despite absolute increases in the concentration of total Hg (Fig. S2) and of the fraction that is cinnabar (Fig. 4). The onset of long-range transport of Hg during the Inca hegemony suggests a shift in Hg extractive technology and associated Hg emissions. Indeed, to transport Hg the ≈ 225 km to Negrilla, at least some emissions must have been in the form of gaseous Hg^0 (or possibly reactive Hg^{2+}). In contrast to coarse particulate cinnabar dust, gaseous atmospheric Hg species can be broadcast atmospherically over far greater distances, can undergo atmospheric oxidation/reduction cycling, and Hg^{2+} can be methylated once delivered to aquatic systems.

A growing number of cores from remote lakes suggest an approximately 3-fold increase in Hg deposition over the last ≈ 100 –150 years (10, 24). These records are predominantly from the northern hemisphere, and do not reveal any significant preindustrial Hg enrichment. In contrast, our results suggest that considerable preindustrial Hg pollution occurred in the Andes. The onset of cinnabar mining at Huancavelica ca. 1400 BC places our lake-sediment records among the earliest evidence for mining and metallurgy in the Andes, of comparable antiquity to the oldest known hammered and annealed objects from well-dated contexts (26). Before Inca control of the mine, Hg emissions appear to have been restricted to the environment surrounding Huancavelica. Over the past ≈ 550 years however, emissions of Hg have been transported long distances.

Materials and Methods

Sediment Geochemistry. Blank values, average relative standard deviations, and recoveries of standard reference materials [NRCC PACS-2 (marine sediment, certified value $3040 \pm 200 \text{ ng g}^{-1}$) and MESS-3 (marine sediment, certified value $91 \pm 9 \text{ ng g}^{-1}$)] associated with DMA80 measurement of Hg are presented in Table S3. Solid-phase Hg thermo-desorption (SPTD) is an indirect method in which Hg species are determined by thermal desorption or decomposition temperatures (9). The method has a detection limit of $0.4 \mu\text{g g}^{-1}$ Hg, and a maximum sample size of ≈ 200 mg. In SPTD analysis, the sample is placed in a quartz furnace and heated at a rate of $0.5 \text{ }^\circ\text{C s}^{-1}$. Volatilized Hg compounds are carried from the furnace with N_2 200 mL min^{-1} , and reduced to Hg^0 by thermal reduction in a quartz tube heated to $800 \text{ }^\circ\text{C}$ before being analyzed by flameless AAS. This method produces temperature-dependent Hg release curves that are species- and matrix-specific. These release curves enable identification of species such as Hg^0 , matrix-bound Hg, and inorganic cinnabar (HgS) by comparison to pure Hg phases and reference materials (Fig. S4). Quantification of Hg species was made by peak integration (27). The sample volume used was between 20 and 200 mg of dry sediment depending on sediment-Hg concentrations. Relative standard deviation on replicate measurements of Hg binding forms in sediments (matrix-bound noncinnabar Hg compounds and cinnabar) of each sample ($n = 3$ –4) ranged 2.8% to 15.4% (mean 8.0%). Total organic matter was determined by loss-on-ignition (28). Sediment chlorophyll a was inferred using visible-near infrared reflectance (VNIR) spectroscopy (29).

ACKNOWLEDGMENTS. We thank W. Hobbs, A. Reyes, J. Vargas, and P. Tapia for assistance in the field; A. Hutchins and S. Castro for assistance in the laboratory; D. Froese, V. St Louis, W. Fitzgerald, and J. Wise for their insightful discussions; and 2 anonymous reviewers. This work was supported by grants from the National Geographic Society, the Geological Society of America, and the Natural Sciences and Engineering Research Council of Canada.

- Burger RL (1992) Chavin and the origins of Andean civilization (Thames and Hudson, London), pp 248.
- Nriagu JO (1994) Mercury pollution from the past mining of gold and silver in the Americas. *Sci Total Environ* 149:167–181.
- Nriagu JO (1993) Legacy of mercury pollution. *Nature* 363:589.
- Wu Y, et al. (2006) Trends in anthropogenic mercury emissions in China from 1995 to 2003. *Environ Sci Tech* 40:5312–5318.

- Wise JM, Féraud J (2005) Historic maps used in new geological and engineering evaluation of the Santa Bárbara Mine, Huancavelica mercury district, Peru. *De Re Metallica* 4:15–24.
- Brown KW (2001) Workers' health and Colonial mercury mining at Huancavelica, Peru. *Americas* 57:467–496.
- McCormac FG, et al. (2004) ShCal04 Southern Hemisphere calibration, 0–11.0 cal kyr BP. *Radiocarbon* 46:1087–1092.

8. Stuiver M, Reimer PJ (1993) Extended ^{14}C database and revised CALIB radiocarbon calibration program. *Radiocarbon* 35:215–230.
9. Biester H, Scholz C (1997) Determination of mercury binding forms in contaminated soils: Mercury pyrolysis versus sequential extractions. *Environ Sci Tech* 31:233–239.
10. Biester H, Bindler R, Martinez-Cortizas A, Engstrom DR (2007) Modeling the past atmospheric deposition of mercury using natural archives. *Environ Sci Tech* 41:4851–4860.
11. Engstrom DR, Balogh SJ, Swain EB (2007) History of mercury inputs to Minnesota lakes: Influences of watershed disturbance and localized atmospheric deposition. *Limnol Oceanogr* 52:2467.
12. Rydberg J, et al. (2008) Assessing the stability of mercury and methylmercury in a varved lake sediment deposit. *Environ Sci Tech* 42:4391–4396.
13. Lockhart WL, et al. (2000) Tests of the fidelity of lake sediment core records of mercury deposition to known histories of mercury contamination. *Sci Total Environ* 260:171–180.
14. Southworth G, et al. (2007) Evasion of added isotopic mercury from a northern temperate lake. *Environ Toxicol Chem* 26:53–60.
15. Burger RL, Mendieta RM (2002) Atalla: A center on the periphery of the Chavín horizon. *Lat Am Antiq* 13:153–177.
16. Rick JW (2004) The evolution of authority and power at Chavín de Huántar, Peru. *Archeolog Pap Amer Anthro Assoc* 14:71–89.
17. Burger RL (2008) in *Handbook of South American Archaeology*, eds Silverman H, Isbell W (Springer, New York), pp 681–703.
18. Onuki Y, Kato Y *Excavations at Kuntur Wasi, Peru: The First Stage 1988–1990*, trans Cooke C (1993) (University of Tokyo Press, Tokyo).
19. Shimada I, et al. (2004) An integrated analysis of pre-Hispanic mortuary practices. *Curr Anthropol* 45:369–402.
20. Petersen U (1989) in *Geology of the Andes and its relation to hydrocarbon and mineral resources*, eds Ericksen GE, Theresa Cañas PM, Reinemund JA (Circum-Pacific Council for Energy and Mineral Resources, Houston), pp 213–232.
21. Cooke CA, Abbott MB, Wolfe AP (2008) Late-Holocene atmospheric lead deposition in the Peruvian and Bolivian Andes. *Holocene* 18:353–359.
22. Shimada I, Epstein S, Craig AK (1982) Batán Grande: A prehistoric metallurgical center in Peru. *Science* 216:952–959.
23. Harris RC, et al. (2007) Whole-ecosystem study shows rapid fish-mercury response to changes in mercury deposition. *Proc Natl Acad Sci USA* 104:16586–16591.
24. Lindberg S, et al. (2007) A synthesis of progress and uncertainties in attributing the sources of mercury in deposition. *Ambio* 36:19–33.
25. Fitzgerald WF, Lamborg CH (2005) Geochemistry of mercury in the environment. *Treatise Geochem* 9:107–148.
26. Aldenderfer M, Craig NM, Speakman RJ, Popelka-Filcoff R (2008) Four-thousand-year-old gold artifacts from the Lake Titicaca basin, southern Peru. *Proc Natl Acad Sci USA* 105:5002–5005.
27. Biester H, Gosar M, Covelli S (2000) Mercury speciation in sediments affected by dumped mining residues in the drainage area of the Idrija mercury mine, Slovenia. *Environ Sci Tech* 34:3330–3336.
28. Heiri O, Lotter AF, Lemcke G (2001) Loss on ignition as a method for estimating organic and carbonate content in sediments: Reproducibility and comparability of results. *J Paleolimnol* 25:101–110.
29. Wolfe AP, Vinebrooke R, Michelutti N, Rivard B, Das B (2006) Experimental calibration of lake-sediment spectral reflectance to chlorophyll a concentrations: Methodology and paleolimnological validation. *J Paleolimnol* 36:91–100.